G&G Lab Notes

EDITORS

Thomas M. Moses   Shane F. McClure | *GIA Laboratory*

DIAMOND

A Rare Fancy Vivid Purple Diamond

In GIA's colored diamond grading system, predominantly purple diamonds can occur in the red-purple, reddish purple, and purple hue ranges. While none of these are common, diamonds in the unmodified purple range are the rarest.

GIA first encountered purple diamonds in the 1970s. Their color is due to plastic deformation of the crystal structure that occurred during their geologic history, resulting in parallel glide planes (referred to as *graining*). This graining exhibits pink and brown dichroism, observed under magnification (see S. Titkov et al., "Natural-color purple diamonds from Siberia," Spring 2008 *G&G*, pp. 56–63). It is extremely rare to see a pure purple hue resulting from such plastic deformation.

Figure 1. This extremely rare 0.81 ct diamond was color graded Fancy Vivid purple.

The New York laboratory recently had the opportunity to examine a 0.81 ct purple diamond with unusually strong color (figure 1). The cut-cornered rectangular modified brilliant was faceted so the graining reflected the purple color throughout the stone, maximizing its intensity. With magnification and diffused lighting, well-defined parallel glide planes were visible through the pavilion (figure 2). These planes showed a strong concentration of purple color, while the surrounding area appeared nearly colorless. The stone fluoresced weak yellow to long-wave UV radiation and was inert to short-wave UV. Under the very strong short-wave UV of the DiamondView, the glide planes displayed clear green fluorescence, which is attributed to the localized distribution of the H3 optical center. The H3 center was also present in the UV-Vis absorption spectrum taken at liquid-nitrogen temperature, along with a strong absorption band centered at ~550 nm, which clearly contributed to the predominantly purple color. FTIR spectroscopy showed the diamond was a type IaA with a very high concentration of aggregated nitrogen, predominantly in the A form. We also noted a very weak absorption at 3107 cm^{-1}, attributed to hydrogen.

The outstanding feature of this diamond was its depth of color, which placed it in the Fancy Vivid range. On the rare occasions the lab has seen purple diamonds, they typically have a dark or unsaturated color, resulting in color grades modified by "gray" or "grayish." It is unusual for GIA to encounter more than a handful of purple diamonds, regardless of their depth of color, in any given year. The rarity is exponentially greater for a diamond with a very strong purple hue.

Jason Darley, Paul Johnson, and John King

Figure 2. The purple coloration in the diamond was concentrated along parallel glide planes. Magnified 60×.

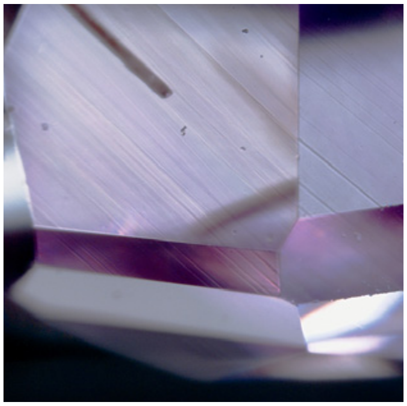

Editors' note: All items were written by staff members of the GIA Laboratory.

Gems & Gemology, *Vol. 47, No. 4, pp. 308–315, http://dx.doi.org/10.5741/GEMS.47.4.308.*

Figure 3. These two diamonds, a 0.85 ct Fancy black heart shape (left) and a 0.20 ct Fancy grayish blue modified pear shape (right), had similar hydrogen-related spectroscopic properties but dramatically different color.

A Strongly Purple-Colored Black Diamond

Hydrogen-rich diamonds with gray to blue to violet colors are rare, but they are well documented in the literature (see, e.g., C. H. van der Bogert et al., "Gray-to-blue-to-violet hydrogen-rich diamonds from the Argyle mine, Australia," Spring 2009 *G&G*, pp. 20–37). The New York lab recently tested such a diamond with an unusually dark tone.

The 0.85 ct type Ia heart shape (figure 3, left) showed extremely strong hydrogen-related features (e.g., 3107 cm^{-1}) in its mid-infrared absorption spectrum. The high concentration of hydrogen produced such a dark appearance that the diamond received a Fancy black color grade.

We compared this heart shape to a 0.20 ct modified pear shape (figure 3, right) with similar overall spectroscopic properties, also type Ia, that received a Fancy grayish blue color grade. In this diamond, however, the hydrogen impurity did not cause such a strong absorption. The difference between the two stones was also clearly displayed in their Vis-NIR absorption spectra in the 400–900 nm range. Both showed typical absorptions for gray to blue to violet diamonds, such as bands near 500 and 700 nm, attributed to hydrogen. The much stronger absorption in the heart shape blocked most of the light return, making it appear virtually black. Its spectrum was very noisy because of the absorbance, and the spectrometer detected only a very weak signal (figure 4). Only with magnification and fiber-optic illumination could we observe fine clouds associated with hydrogen in such diamonds (figure 5); the stone's true deep purple bodycolor was also seen.

This rare diamond provides a good example of an extreme end of the color range of hydrogen-rich diamonds, in which the purple color was so deep that the stone appeared black.

Paul Johnson

Figure 4. The Vis-NIR absorption spectrum of the Fancy black heart shape showed a weak signal and significant noise.

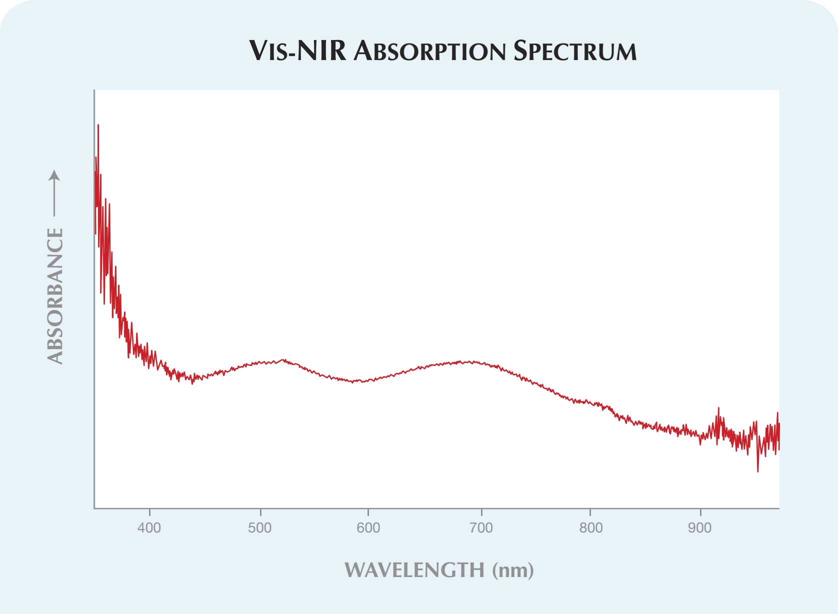

Figure 5. With magnification and fiber-optic illumination, the heart-shaped diamond's deep purple bodycolor became apparent.

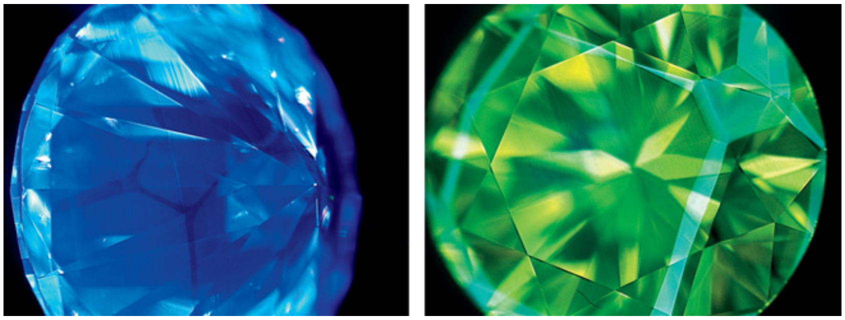

Figure 6. In the DiamondView, this 0.99 ct HPHT-treated diamond (left) shows four-fold symmetry that appears similar to the cross pattern typically encountered in HPHT synthetics (right, 1.00 ct).

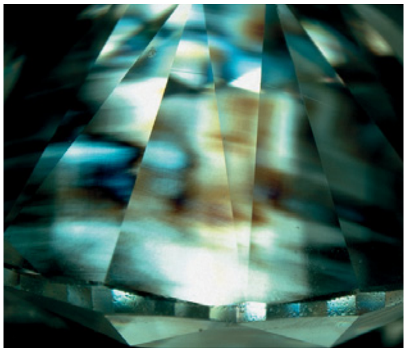

Figure 7. The HPHT-treated diamond's mottled strain pattern indicated natural origin. Image width: 4.35 mm.

HPHT-Treated Diamond with the Fluorescence Pattern of an HPHT-Grown Synthetic

Synthetic diamonds grown at high-pressure, high-temperature (HPHT) conditions are no longer rare in the market. One method to distinguish them from natural diamonds is imaging their growth patterns with ultraviolet-activated fluorescence, such as with the DiamondView instrument.

The growth structure of HPHT synthetics is typically quite distinctive and, in most cases, eloquently displayed in their fluorescence images. Because HPHT synthetic diamonds form under different conditions than their natural counterparts, the growth rates of their various crystal faces are generally quite different. The resulting morphology of HPHT products is typically cubo-octahedral, whereas natural diamonds grow as octahedra. The overwhelming majority of HPHT synthetics show a diagnostic cross shape in their luminescence pattern. Sometimes, however, natural diamonds exhibit four-fold symmetry that may be confused with this cross pattern.

One such instance was seen recently in the Carlsbad laboratory. A 0.99 ct F-color type IIa round brilliant underwent advanced testing to determine if it was natural, treated, or synthetic. The stone's DiamondView image (figure 6, left) showed a configuration resembling the cross pattern (figure 6, right), and its photoluminescence (PL) spectra indicated the sample had been subjected to HPHT conditions, therefore suggesting it was an HPHT-grown synthetic. Nevertheless, microscopic examination with crossed polarizers revealed a mottled strain pattern typical of natural type IIa diamonds (figure 7), and additional peaks in the PL spectra confirmed it was an HPHT-treated natural diamond.

DiamondView imaging can be diagnostic for synthetic diamonds, particularly those of HPHT origin. But careful consideration of both DiamondView images and spectral data (particularly PL) is usually necessary to definitively identify natural or synthetic origin. The cross-shaped growth pattern in the present diamond may be due to formation under different conditions (i.e., lower temperatures) than those typically experienced by natural diamonds, which led to its altered morphology. The fact that this diamond was chosen for HPHT treatment was an interesting coincidence.

Sally Eaton-Magaña

Type IIb Diamond with Long Phosphorescence

It is well known that type II synthetic diamonds and some natural diamonds (including type IIb) are phosphorescent. In natural diamonds the effect usually lasts for only a few seconds. However, a 4.23 ct emerald cut (figure 8) recently submitted to the Carlsbad laboratory proved to be an exception. Identified as an untreated type IIb diamond with D color and IF clarity, it

Figure 8. This 4.23 ct type IIb diamond is shown before (left) and after (right) exposure to short-wave UV radiation for 10 seconds. The photo on the right shows the diamond's strong blue phosphorescence.

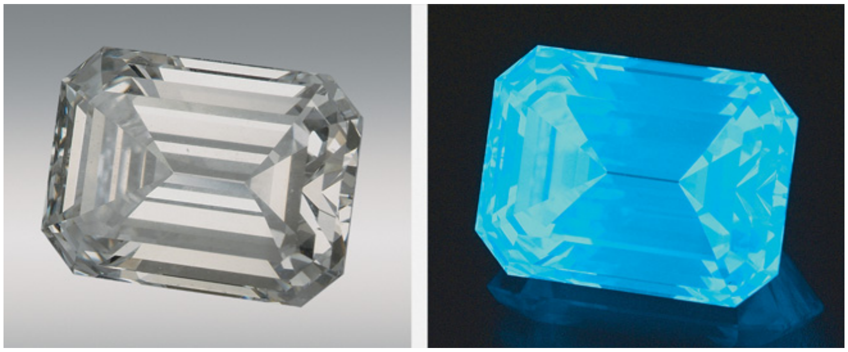

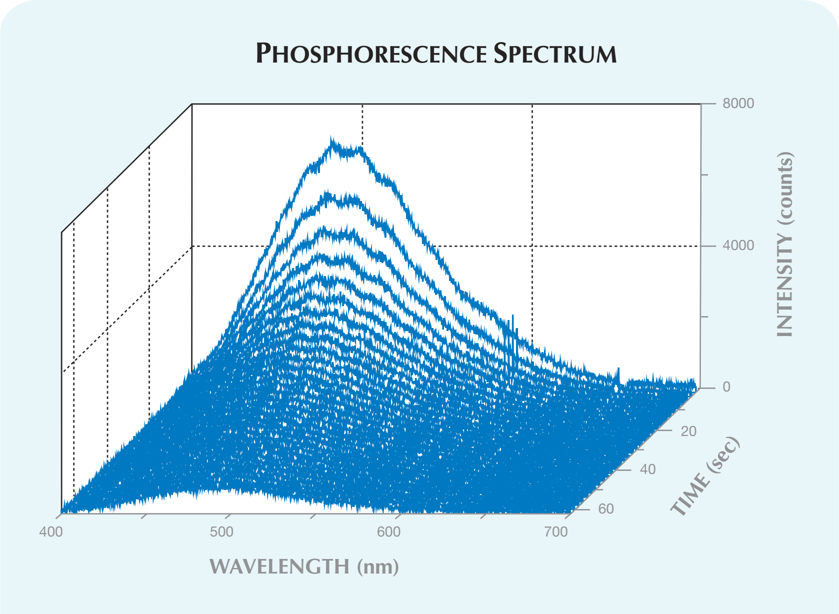

Figure 9. The three-dimensional spectral plot for the diamond in figure 8 shows its long-lasting phosphorescence corresponding to the 500 nm band. The diamond was exposed to UV radiation for 20 seconds and data were collected over one second intervals.

displayed very weak to weak greenish blue fluorescence to long- and short-wave UV radiation. During UV exposure, the fluorescence appeared to intensify due to the sample's strong phosphorescence. After 5 seconds of exposure to short-wave UV radiation, the diamond displayed bright blue phosphorescence (see video in the *G&G* Data Depository at gia.edu/gandg), and it continued to luminesce for several minutes.

Phosphorescence spectroscopy revealed a band at 500 nm (also documented in type IIb diamonds by S. Eaton-Magaña et al., "Luminescence of the Hope diamond and other blue diamonds," Fall 2006 *G&G*, pp. 95–96) that was responsible for the blue phosphorescence. Figure 9 shows the spectra collected over a period of 60 seconds in a three-dimensional plot. At the end of 60 seconds, the 500 nm phosphorescence band was still visible. The calculated half-life of this band was 8.4 seconds. By comparison, the Hope diamond's 500 nm band half-life is only 1.8 seconds (S. Eaton-Magaña et al., "Using phosphorescence as a fingerprint for the Hope and other blue diamonds," *Geology*, Vol. 36, No. 1, 2008, pp. 83–86). Figure 10 shows the relationship between apparent bodycolor and phosphorescence half-life in 300 natural type IIb diamonds examined in the GIA laboratory. The present diamond's 500 nm band had a much longer half-life and a stronger intensity than most natural type IIb diamonds; this combination produced the unusually long phosphorescence.

This diamond also exhibited thermoluminescence, as described in the Spring 2011 Lab Notes (pp. 50–51). It was immersed in a liquid-nitrogen bath (–196°C) and simultaneously exposed to short-wave UV. After removal from the bath, it warmed up rapidly and displayed a flash of blue thermoluminescence. After a few seconds of additional warming, it exhibited the long-lasting phosphorescence described above. A second video documenting both luminescence behaviors is available in the *G&G* Data Depository.

Andy H. Shen and
Sally Eaton-Magaña

Figure 10. Data compiled for 300 natural type IIb diamonds show variations in the average half-life of phosphorescence bands (with error bars showing standard deviations) at 500 and 660 nm according to their bodycolor. Colorless type IIb diamonds generally do not show a red phosphorescence band at 660 nm, and their blue 500 nm band has a long half-life. Type IIb diamonds with stronger blue coloration have both 500 and 660 nm bands, and the half-life of their blue phosphorescence is much shorter.

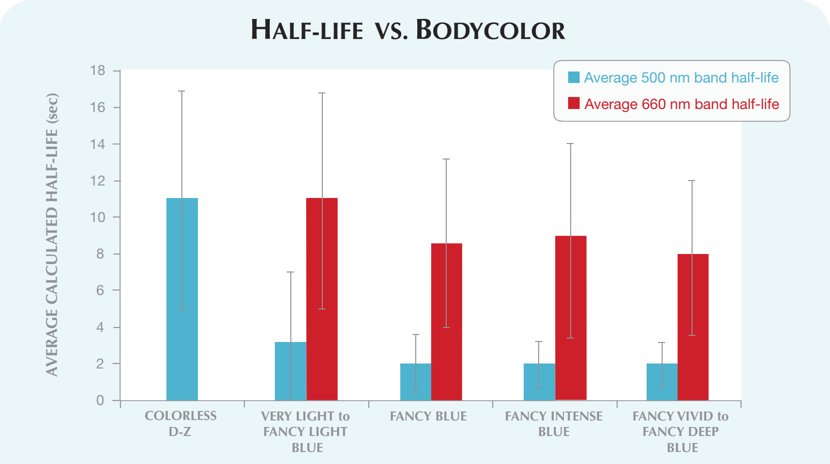

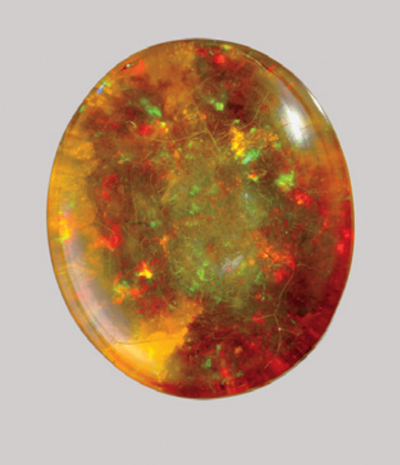

Figure 11. This 67.17 ct opal was clarity enhanced with some type of oil.

OPAL

Clarity-Enhanced, with Artificial Matrix

The Carlsbad laboratory recently received a 67.17 ct opal cabochon (figure 11) for identification. The stone showed an orangy yellow bodycolor and moderate play-of-color. It also had an unusual mottled gray "matrix" on the back and felt slightly greasy to the touch. In reflected light, a network of fine lines on the surface revealed a large amount of crazing, but these lines were not easily seen upon initial examination.

Gemological examination produced measurements consistent with natural opal. The refractive index was 1.45, but we did not test specific gravity because of the presence of the "matrix." The sample was inert to long-wave UV radiation and gave a weak greenish yellow reaction to short-wave UV. Notably, the fractures fluoresced weak yellow to both long- and short-wave UV.

Microscopic examination revealed a somewhat columnar structure and bodycolor similar to material from Wollo Province, Ethiopia. A dense network of very low-relief fractures was also seen throughout the stone; their subtle appearance immediately suggested clarity enhancement. Closer examination showed flattened gas bubbles in many of the fractures from incomplete filling (figure 12, left). When exposed to a relatively low temperature thermal probe, the fractures began to sweat (figure 12, right). Because of the mobile nature of the clarity enhancing substance, we concluded that the stone was treated with some variety of oil rather than an epoxy resin.

The "matrix" on the back of the cabochon consisted of a hard gray resin-like material that showed swirl marks and also some grinding marks, indicating it had been applied during or after the lapidary process. This layer added significant weight and likely helped hold the highly fractured stone together.

While we do not know for certain if this stone was from the Wollo deposit, this seems likely given its appearance and the high volume of material recently mined there. Although this opal did not show hydrophane character, in one of these contributors' (NR) experience, not all Wollo opal is hydrophane type. In addition, some of the orangy yellow Wollo opal seems to be prone to crazing.

As with any new source, artificially enhanced lesser-quality material will eventually make its way to the market as treatments are developed to create salable products. Even though very high-quality untreated Ethiopian opal is readily available, buyers should be aware that an increasing amount of treated material is appearing in the trade, including clarity-enhanced samples such as this one and others subjected to forms of color modification (see, e.g., N. Renfro and S. F. McClure, "A new dyed purple opal," www.gia.edu/research-resources/news-from-research). As with all treatments, these are acceptable as long as proper disclosure is given to the buyer.

Nathan Renfro and Phil York

Figure 12. Low-relief fractures were seen throughout the opal, many of which showed flattened gas bubbles near the surface (left). Droplets of oil readily sweated out of the fractures when exposed to low temperature heat from a thermal probe (right, reflected light). Magnified 40×.

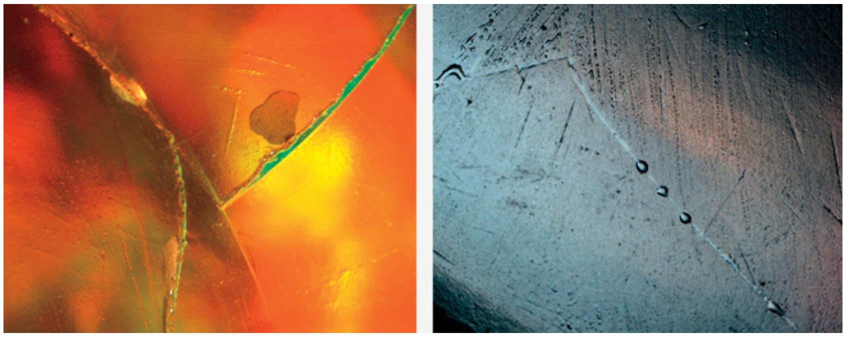

Ethiopian Black Opal

The Carlsbad laboratory recently examined a 10.67 ct black opal (figure 13), reportedly from the Wollo Province of Ethiopia. Because black is not a common bodycolor for opal from this important locality, and there are increasing reports of this material being treated (e.g., the article by N. Renfro and S. F. McClure in this issue, pp. 260–270), we sought to determine the cause of color in this sample. Also submitted was an approximately 1 kg parcel of opal nodules, on which the client permitted destructive testing to investigate the cause of the bodycolor.

Standard gemological properties from the cabochon were consistent with those expected for opal, including an RI of 1.45 and a hydrostatic SG of 2.05. It was inert to long- and short-wave UV radiation. Microscopic examination revealed small brown dendritic inclusions, a "digit-pattern" columnar structure, and nonphenomenal potch areas with a greenish cast. These microscopic observations and physical properties are consistent with features seen in other colors of Wollo opal.

The rough material had the same general appearance and gemological properties as the cabochon, except that the nodules displayed color zoning. One of the rough pieces was sliced in half, revealing a dark brown to black core with a light brown to near-colorless perimeter (figure 14). This structure suggested natural color, as the reverse pattern (dark perimeter with light core) would be expected if the dark color had been artificially introduced.

We performed LA-ICP-MS chemical analysis of one slice, and Mn was the only element that showed distinct variations between the dark core (average 261 ppmw) and light rim (average 23 ppmw). The elevated Mn in the core is consistent with the dark color, as black manganese oxides have been observed on Wollo opal. If Mn was present during opal formation, it is reasonable to conclude that manganese oxides would be incorporated into the opal and impart a dark bodycolor. Qualitative analysis by EDXRF also showed relatively high levels of Mn when compared to a white opal from Wollo.

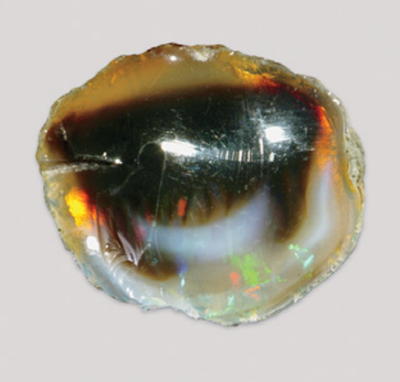

Figure 14. This 8.37 ct slice from a black opal nodule shows a dark core with a near-colorless to light brown perimeter, suggestive of natural color. LA-ICP-MS analysis of the core revealed high concentrations of Mn, which is responsible for the bodycolor.

While treated black Ethiopian material has been documented (e.g., www.stonegrouplabs.com/SmokeTreatmentinWolloOpal.pdf), opal enthusiasts will certainly appreciate these natural-color gems from the Wollo Province.

Nathan Renfro

Coated Bead-Cultured Freshwater PEARLS

In September 2011, a strand of unusually large white baroque "pearls" was submitted to the New York laboratory for identification. The 17 pieces measured 22.43 × 17.60 × 14.17 mm to 29.46 × 19.64 × 16.50 mm. They had a noticeably unnatural color and surface appearance, yet their baroque shape was typical of some freshwater cultured pearls seen in the marketplace (figure 15).

Microscopic inspection revealed a surface structure that lacked the characteristic platelet structure of nacreous pearls. Instead, the surfaces had a "glittery" painted appearance and unnaturally distributed orient, fea-

Figure 13. This 10.67 ct opal cabochon is reportedly from the Wollo Province of Ethiopia. The black bodycolor is caused by natural manganese oxides incorporated during formation.

Figure 15. This strand contains 17 large (up to 29.46 mm), coated, baroque-shaped, bead-cultured freshwater pearls.

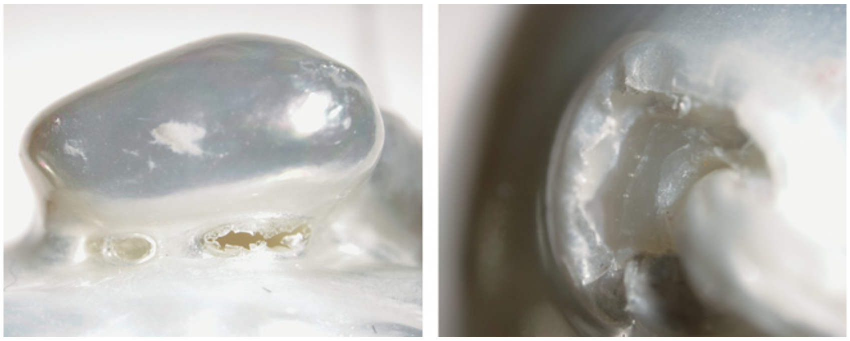

Figure 16. Microscopic examination of the cultured pearls reveals air bubbles trapped in folds within the surface (left, magnified 20×). A close-up of a drill hole shows puckering and peeling of the outer surface, as well as the underlying nacreous surface of the cultured pearl (right, magnified 20×).

tures commonly found in imitation pearls. Also, air bubbles were trapped in the folds and crevices throughout the strand (e.g., figure 16, left). Puckering at the drill holes, as well as noticeable chipping and peeling, further indicated a pearl imitation. In addition, some of the drill holes revealed an underlying nacreous layer (figure 16, right). These observations suggested the strand consisted of nacreous pearls with a thick coating, which would explain their organic-appearing shape despite their artificial appearance.

Most of the samples showed obvious uniformly round bulges like those seen in baroque bead-cultured pearls. Examination of these areas with fiber-optic lighting showed distinct banding that is typical of shell beads. X-radiography revealed that the entire strand was indeed bead cultured (figure 17). No distinct boundary between the very thin nacre and the coating could be observed in the X-ray images.

The long-wave UV reaction was relatively inert across the body of the cultured pearls but strong bluish white along the narrower areas where the coating was most concentrated. When exposed to X-rays, the strand showed moderate yellow luminescence (which was visible through the coating), typical of a freshwater origin. This was confirmed by LA-ICP-MS chemical analysis of an exposed nacreous layer, which showed high concentrations of Mn and Sr. Both EDXRF and LA-ICP-MS detected significant amounts of bismuth in the coating. Bismuth is often used in artificial coatings to create a pearlescent appearance (J. V. Koleske, Ed., *Paint and Coating Testing Manual: 14th Edition of the Gardner-Sward Handbook*, American Society for Testing and Materials, Philadelphia, 1995, pp. 229–230). Natural saltwater pearls with a bismuth-bearing coating were reported in a Fall 2005 Gem News International entry (pp. 272–273).

This strand proved unusual for two reasons: Bead-cultured freshwater pearls are not common in the market, and the pearl coatings we have examined have tended to consist of clear silicone polymers applied to improve luster or protect the underlying nacre (see Lab Notes: Spring 2000, p. 65; Spring 2002, pp. 83–84). The coating on the present strand created the illusion of thick, luminous nacre, and was probably applied to reinforce the precariously thin nacre layer on these cultured pearls.

Akira Hyatt

Figure 17. X-radiography of the strand reveals a bead-cultured structure and very thin nacre layers around the beads.

Tenebrescent ZIRCON

Only a few gem varieties are known to exhibit reversible photochromism, also known as tenebrescence. This phenomenon is most notable in hackmanite a variety of sodalite. Recently we learned about another gem showing tenebrescence: zircon. Our source indicated that five such stones had been discovered approximately 25 years ago in central Australia. When left in the dark for a few hours, the specimens reportedly turned orange, which would fade to near-colorless within a few minutes of exposure to light (figure 18).

Two of the Australian samples were provided for examination in September, 2011: a 3.07 ct piece of rough and a 1.80 ct faceted round brilliant. Both samples had fairly typical properties for zircon: RI—over the limits of the refractometer (>1.81); SG—4.72; and fluorescence—very weak orange to long-wave UV radiation, and moderate orangy yellow to short-wave UV. Microscopic examination revealed reflective disk-like inclusions. LA-ICP-MS chemical analysis did not show anything out of the ordinary for zircon.

When first taken out of the dark environment, the stones were orange.

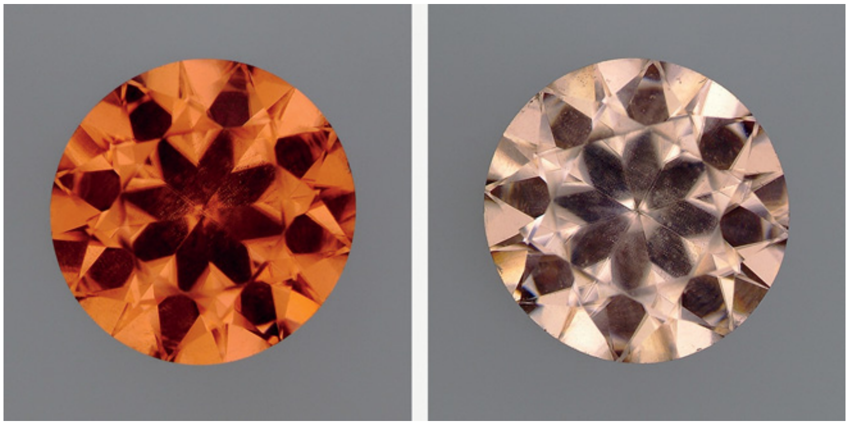

Figure 18. This 1.80 ct tenebrescent zircon is shown just after it was taken out of the dark (left), and after exposure to a fiber-optic light for several minutes (right).

Placed under a standard 13.3 watt incandescent desk lamp, they faded within a couple of minutes to a light, slightly pinkish brown. The color did not appear to change any further under indirect office lighting. Additional exposure to a 150-watt fiber-optic light for approximately one minute caused them to fade to pale pinkish brown. Longer exposure to the fiber-optic light did not cause any more fading. After being stored in the dark overnight, the stones returned to their original color. We repeated this process several times with the same results.

Some tenebrescent stones change back to their original color by exposure to short-wave UV radiation or heat. Attempts to restore the orange color of these zircons with short-wave UV were unsuccessful. We also tried low heat without success, but this may be because the samples were not heated enough; they were not heated further out of concern for potential damage.

A search of the literature by GIA's Richard T. Liddicoat Library and Information Center found no mention of "tenebrescent" zircon, although several books described zircons with such behavior. The oldest reference found was in Max Bauer's *Precious Stones* (1904), which noted: "Zircon—The colour and luster of some hyacinths [probably referring to brownish or pinkish orange material] is liable to change even at ordinary temperatures if the stones are exposed to light. . . . In some cases the colour becomes pale. . . . Such altered stones, if kept in darkness, will recover their original colour. . . ." Interestingly, several other references gave fairly similar descriptions of this phenomenon, but it was never referred to as tenebrescence—even though it fits the definition. Likewise, a Fall 1986 Lab Note (pp. 188–189) documented reversible color-change in a blue zircon, which changed to an undesirable grayish brown with exposure to long-wave UV radiation.

Several online retailers are selling this material as tenebrescent zircon. The stones are reported to be from Tanzania, Australia, Cambodia, or Nigeria; one site says it was found 10 years ago. It remains unclear whether any of this information is reliable, but one thing is certain: tenebrescent zircon exists, and it is a wonder that this interesting material has been so little reported in the contemporary literature.

Shane F. McClure

PHOTO CREDITS
Sood Oil (Judy) Chia—1; Paul Johnson—2 and 5; Jian Xin (Jae) Liao—3 and 15; Sally Eaton-Magaña—6; David Nelson—7; C. D. Mengason—8 and 18; Robison McMurtry—11, 13, and 14; Nathan Renfro—12; JaeWon Chang—16.